Mixing Control in a Plane Shear Layer

K. Z. Korczak* and R. A. Wessel†
Case Western Reserve University, Cleveland, Ohio

An investigation of mixing processes in a plane shear layer by a direct numerical simulation with a high-order numerical technique, the isoparametric spectral element method, is presented. The computational domain includes a region with the splitter plate where two laminar (Blasius) boundary layers with different velocities and concentrations merge to form the shear layer and a downstream region where the flow undergoes transition to highly unsteady structures with intensive mixing. The augmentation of mixing as a function of a downstream location and the intensity and type of vortical structures in the layer are investigated by an introduction of disturbance at the high-velocity inflow. The character of the dynamic mixing is displayed along with time-averaged profiles and statistical characteristics.

Introduction

THE fundamentals of plane mixing layers have been the subject of extensive theoretical, experimental, and numerical investigations due to their relative "simplicity," common technological occurrences, and a significant importance in mixing processes, often combined with chemical reactions and combustion. Studies have been focused on the basic mechanisms responsible for the characteristic vortex structures in the layer and their relation to the mixing and chemical processes.

The bulk of the research effort has been primarily experimental.[1-9] Some attempts have been made to use numerical simulations of the linearized Navier-Stokes equations[10-12] and the inviscid Euler equations.[13] With the progress in computer technology paralleled by significant developments in numerical algorithms, a direct simulation of the full Navier-Stokes equations has become possible. Among many numerical techniques used in varieties of flow simulations, high-order methods seem to be the only *realistic* candidates for highly unsteady and turbulent flows. Algorithms based on spectral expansions[14] have been used in testing of turbulent theories[16-18] and in validation studies for turbulent wakes,[19] mixing layers,[20-22] chemically reacting turbulent mixing layers,[23,24] etc.

Turbulent mixing layers are strongly influenced by large-scale vortex structures generated by instabilities and rolling effects of the velocity difference. Those structures, very active as they move along, typically merge in larger vortex lumps dominating the flow.[1,2] For moderate Reynolds numbers, the developments are two-dimensional in character. Above that range, secondary instabilities initiate developments of long longitudinal structures,[3] and the flow exhibits three-dimensional behavior.

A thorough understanding of the basic mechanisms governing and controlling the vortex structures is important because they are responsible for a substantial augmentation of mixing in the layer. The mixing process could be seen as a combination of three components:[5] 1) tongues of unmixed fluid transported across the layer by large-scale motions, 2) interfacial diffusion zones of finite thickness separating the zones of unmixed fluid, and 3) cores of mixed fluid of nearly homogeneous composition corresponding to the vortex lumps. The entrainment of fluid into the shear layer has been observed to be asymmetric with dominance of the high-speed fluid. As a consequence, the average composition of the core of a mixed fluid is directly related to (approximately equal to) the value of the corresponding entrainment ratio.[5,6] Several investigators[5-9] have made an effort to relate the extent of the entrainment asymmetry to the concentration probability density function (p.d.f.) and have developed simple models to characterize the mixing process.[25]

Direct numerical simulations, by supplying complete flowfield data and allowing detailed examination of the flow process, can potentially give valuable insights. Because of the highly unsteady or turbulent nature of such flows, the numerical algorithm has to resolve small scales of motion without introducing significant artificial dissipation or diffusion. Traditional spectral methods have been successfully used for that purpose.[19-21,23] However, the success of those approaches has been limited to simple geometries and periodic flows that allow only temporal growth. In an arbitrary (general) case, a global spectral technique fails to provide the flexibility required to simulate practical flow situations.

One path adopted by some researchers has been to implement spectral expansions in vertical and spanwise directions of a shear layer, resolving the remaining flow direction with finite differences.[24] This approach allows simulations of flow developments in both space and time. However, there are two limitations associated with this technique.

First, the accuracy of the solution could be dominated by the finite-difference errors, particularly for mixing or chemical reactiaons. Looking at the characteristic structures that evolve during mixing in the shear layer, it is clear that, in the vicinity of vortex roll ups, the gradients of concentration are large in all directions, not only in the vertical one. This results in potentially significant numerical errors that contaminate the data. Second, the spectral expansions used in such schemes require geometric continuity in the vertical direction. As a consequence, the shear layer flow has to be initiated downstream from the edge of the splitter plate. This, in turn, requires proper prediction of the inflow profile. It has been shown[22] that correct prediction of that profile is practically impossible (unless the Reynolds number is quite small) because the effects of the splitter plate on the flow do not dissipate quickly and the flow never reaches a uniform steady profile. The inflow conditions affect the whole flowfield, and an error there could significantly alter the nature of the flow.

A different approach[22] has been implemented to remedy the

Received Feb. 1, 1988; revision received April 25, 1989.

*Assistant Professor, Department of Mechanical and Aerospace Engineering. AIAA Associate Member.

†Graduate Student, Department of Mechanical and Aerospace Engineering.

preceding problems with the help of the isoparametric spectral element method,[26] an algorithm based on spectral and finite-element methods. This approach tolerates geometric singularities and arbitrary boundary conditions, while preserving high-order accuracy and creating an opportunity to simulate a realistic (minimal intervention) mixing-layer flow. The numerical formulation permits simulation of a shear layer that starts as two (Blasius) boundary layers around a splitter plate which merge downstream of the edge of the plate.[22] That study clearly shows that the flow in the layer becomes unsteady before a uniform and steady velocity profile has a chance to develop. The imposition of correct and unique inflow boundary conditions combined with the accuracy of the numerical algorithm have made it possible to study initial formations and developments of vortex structures.

The present study is a continuation of the previously mentioned investigation[22] and concentrates on the mixing process in the shear layer and means of influencing and controlling the intensity of it.

Problem Definition

A plane mixing layer is typically formed by two boundary-layer flows with different mean velocities originating on both sides of a splitter plate and merging from its edge downstream. In the case of a constant density and viscosity, the flow is uniquely described by the general incompressible Navier-Stokes equations,

$$\frac{\partial v}{\partial t} = v \times \omega - \nabla \Pi + \frac{1}{Re} \nabla^2 v \qquad \text{in} \qquad \mathfrak{D} \tag{1}$$

where $v(x,t)$ $(= u\hat{x} + v\hat{y} + w\hat{z})$ is the velocity, $\Pi(= p + 1/2v \cdot v)$ is the dynamic pressure, $\omega(x,t)$ $(= \nabla \times v = \omega_1\hat{x} + \omega_2\hat{y} + \omega_3\hat{z})$ is the vorticity, Re is the Reynolds number, and $\mathfrak{D}$ is the flow domain. For two-dimensional applications, w velocity component as well as ω_1 and ω_2 are identically equal to zero.

We assume that the upper, high-speed, pure fluid mixes with a different low-speed fluid. Based on the assumption that the changes in concentration do not interfere with the velocity field, the mixing of the high-speed fluid could be described in terms of the passive scalar equation,

$$\frac{\partial \xi}{\partial t} + v \cdot \nabla \xi = \frac{1}{Re \cdot Sc} \nabla^2 \xi \qquad \text{in} \qquad \mathfrak{D} \tag{2}$$

where $\xi(x,t)$ is the concentration of the high-speed fluid, Re is the Reynolds number of the flow (defined below), and Sc is the Schmidt number, $Sc = \nu/D$, with D being the coefficient of diffusivity for the passive scalar. It is assumed that the diffusion of the passive scalar obeys Fick's law and that the coefficient of diffusivity D is invariant with respect to time and space.

We conduct a numerical experiment, a direct simulation of Eqs. (1) and (2) with the isoparametric spectral element method[26] for 2D flows in a domain shown on Fig. 1. The computational region, with the end section of the splitter plate included, allows the flow to begin as laminar (Blasius) boundary layers (on both sides of the plate) and to undergo transition to turbulence downstream. This ensures a realistic initiation of the flow, removing the possibility of influencing the formation of vortex structures by inflow conditions. Above and below the mixing region freestream velocities are assumed and the outflow conditions are imposed as natural boundary conditions.

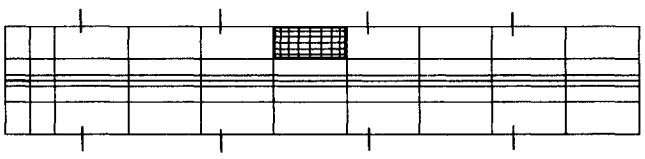

Fig. 1 Two-Dimensional geometry,. The rectangles represent elements, each with a local mesh (11 × 9) the same as shown. (Elements' positions: x = 0,5, 10, 25, 40, 55, 70, 85, 100, 115, and 130; y = −10, −4, −1, 0, 1, 4, and 10). The thick line at $y = 0$, x = 0–5 indicates the splitter plate. The tic marks indicate cross sections for statistical data.

The domain (Fig. 1) with 60 macroelements, each with a 11 × 9 local mesh, provides a mesh-point density "proportional" to the complexity of the flow, resulting in high resolution around the splitter plate and in the wake region. The mesh extends from −10 to 10 units in the y direction and 130 units in the x direction. The splitter plate is positioned at $y = 0$ from x = 0–5.

The flow, driven with upper freestream velocity $U_t = 1$ and lower $U_b = 0.5$, has an initial boundary-layer thickness $\delta = 0.9$ on both sides of the plate. At the edge of the plate ($x = 5$), the theoretical combined thickness of both streams, $\delta_t = 2.48$, is assumed to be the characteristic length for the flow in the y direction. The velocity difference, $\Delta U = U_t - U_b$, is taken to be the characteristic velocity, and the Reynolds number is defined in terms of the above, $Re = \delta_t \Delta U/\nu$.

For the passive scalar equation [Eq. (2)], the concentration for the high-speed fluid at the inflow above the splitter plate and along the upper boundary is assumed to be equal to 1. For the low-speed fluid the concentration at the inflow below the splitter plate and along the lower boundary is fixed at 0. At the outflow and on the splitter plate, natural (0 flux) boundary conditions are imposed.

Velocity fluctuations are recorded at six different locations along the layer: $y = 0.5$ and x = 17.5, 32.5, 47.5, 62.5, 77.5, and 92.5. The simulations are conducted for one case with uniform inflow boundary conditions and several cases with forced oscillations introduced into the upper velocity profile at inflow:

$$u_{\text{in}} = u_{\text{Blas}} + A_f 3 \sin(\pi y/2) \sin(2\pi f_f t)\, e^{-1.5y} \tag{3}$$

where A_f is the maximum amplitude and f_f the frequency of the forcing component. The forcing is applied only in the vicinity of the boundary layer and decays exponentially to 0 for y approaching the upper boundary. The Reynolds number for all simulations is kept constant at $Re = 250$.

Statistical analysis of the mixing process is based on the p.d.f. of the high-speed fluid concentration $\xi(x,y,t)$ measured at four cross sections located at x = 15.2, 45.2, 75.2, and 105.2 (Fig. 1). The pdf of ξ at a given point y for a fixed cross section is denoted as $p(\xi,y)$[6] and defined such that $p(\xi_0)\, d\xi$ is the probability of finding fluid with concentration ξ where $\xi_0 < \xi < \xi_0 + d\xi$. The interval of ξ, $0 \le \xi \le 1$, has been divided into 50 subintervals for numerical sampling. The unmixed low-speed fluid corresponds to $\xi = 0$, and a pure high-speed fluid corresponds to $\xi = 1$.

We can characterize the mixed-fluid p.d.f. by its area and first moment.[6] The area of the p.d.f., P_m, expresses the total probability of finding *mixed* fluid at *any* concentration and is given by

$$P_m(y) = \int_{\epsilon}^{1-\epsilon} p(\xi,y)\, d\xi \tag{4}$$

The integration excludes the regions of unmixed fluids located at the ends of the $p(\xi,y)$ spectrum within a region of thickness ϵ equal to the size of the elementary subinterval mentioned earlier. A value of $P_m(y)$ of less than unity signifies the presence of unmixed fluid.

The first moment of $p(\xi,y)$, called the average mixed-fluid concentration, is given by

$$\xi_m(y) = \frac{\int_{\epsilon}^{1-\epsilon} \xi \cdot p(\xi,y)\, d\xi}{\int_{\epsilon}^{1-\epsilon} p(\xi,y)\, d\xi} = \frac{\int_{\epsilon}^{1-\epsilon} \xi \cdot p(\xi,y)\, d\xi}{P_m(y)} \tag{5}$$

The function is used to define the total mixed-fluid concentration for an entire cross section of the flow:

$$\xi_M = \frac{\int_{-\infty}^{+\infty} P_m(y)\xi_m(y)\,dy}{\int_{-\infty}^{+\infty} P_m(y)\,dy} \tag{6}$$

Based on the preceding quantity, we define the entrainment ratio E for a given cross section as

$$E = \frac{\xi_M}{1 - \xi_M} \tag{7}$$

In all of the previous definitions, the vertical distance y is measured with respect to the splitter plate position. For all plots, however, the coordinate y is substituted with a normalized coordinate $y/(x - x_0)$. Here, x is the position of a given cross section and x_0 is the origin of the unforced mixing layer. In our case, x_0 has been determined to be approximately equal to -7.

Numerical Method

The 2-D isoparametric spectral element method,[26] a high-order finite-element technique, divides the domain into a series of quadrangular elements transformed into regular squares. All functions (including the geometric transformation) are represented as tensor-product high-order Lagrangian interpolants through Gauss-Lobatto-Chebyshev (or Legendre) collocating points. The method incorporates a splitting scheme that effectively separates the nonlinear, pressure, and viscous parts of the general incompressible Navier-Stokes equations [Eq. (1)]. An explicit standard collocation approach with third-order Adams-Bashforth is used for the nonlinear terms. The remaining pressure and viscous parts are solved implicitly with variational projection operators based on Chebyshev (or Legendre) polynomial expansions. Similarly, the convective and dissipative terms in the passive scalar equation [Eq. (2)] are separated and solved as indicated earlier.

For a 2-D algorithm in a supercomputer environment, the most efficient and accurate solver is a direct matrix inversion with static condensation. Fast iterative solvers (conjugate gradients and others) have been used on other occasions. Both the direct solver and the conjugate gradients solver allow efficient vectorization and solution of the elemental matrix systems in parallel. These factors enable the technique to be particularly well suited for modern supercomputers.

Unforced Simulation

The simulation is conducted in a geometric setup (Fig. 1) allowing an investigation of the origin of the mixing layer and its early formations and growth over a distance of $\simeq 50$ initial (at the splitter edge) mixing-layer thicknesses at $Re = 250$. For the purpose of this investigation, the Schmidt number is assumed to be $Sc = 0.5$. As initial conditions, flow and concentration data from previous simulations are used, and the simulations are carried on for a long time (20,000 steps, $\simeq 500$ time units) to diminish the influence of transients due to initial conditions on the final analysis.

At six locations in the mixing layer at constant $y = 0.5$ and $x = 17.5$, 32.5, 47.5, 62.5, 77.5, and 92.5, u-velocity has been recorded for determining the natural (unforced) frequency response of the flow system. A Fourier transform of those velocity fluctuations reveals the full frequency spectrum as shown on Fig. 2. The detected frequencies in this flow practically do not exist above 0.20 Hz. The maximum detectable frequency (based on the time step $\Delta t \simeq 0.025$) is about 10 Hz, well above the existing spectrum. For the given Reynolds number, the flow does not exhibit any rapid developments, as seen on Fig. 2. The strength of the spectrum is increasing downstream, and the characteristic drifting toward lower frequencies[1,22] is clearly visible.

The evolving vortex structures in the flow are plotted on Fig. 3. As mentioned earlier, the flow development is laminar

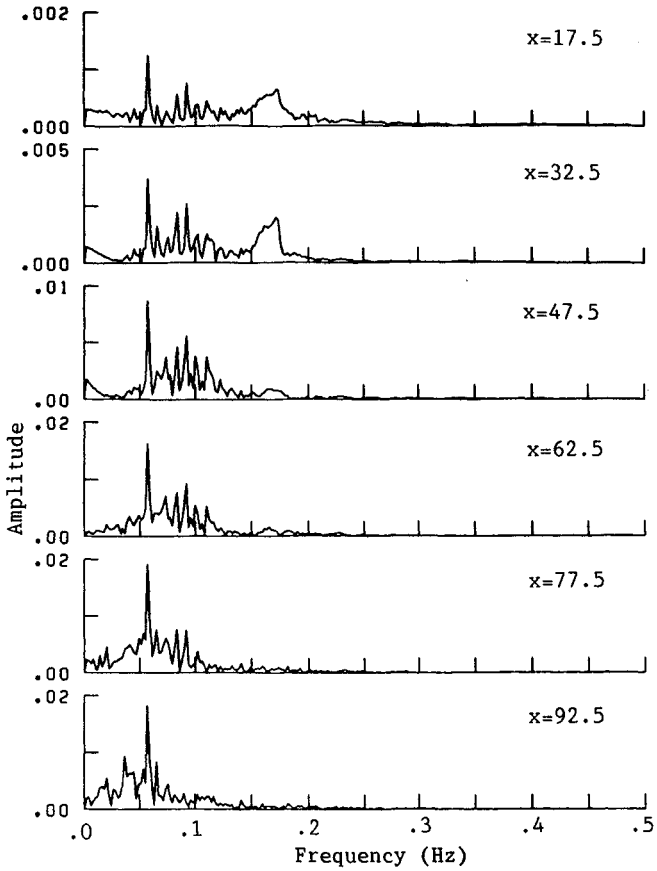

Fig. 2 Frequency plots for unforced case; $Re = 250$. Fourier transform of velocity fluctuations measured at $y = 0.5$ and corresponding x locations.

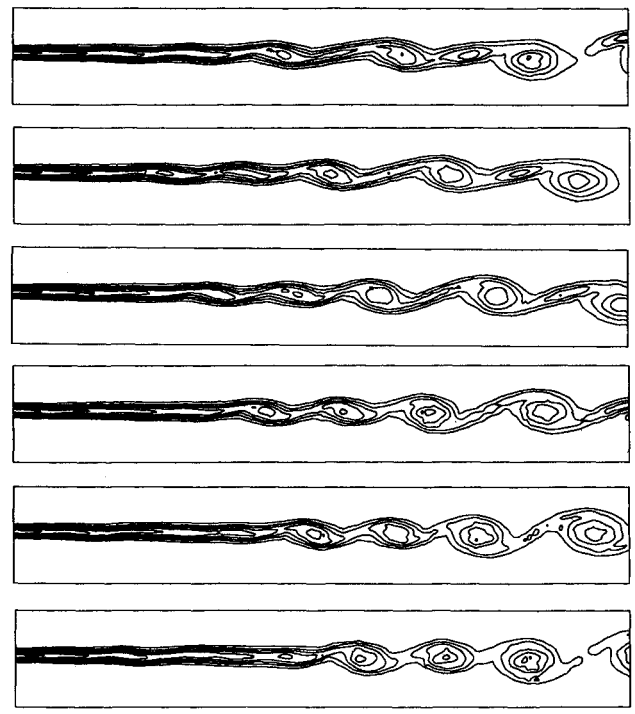

Fig. 3 Vorticity contours for unforced case; $Re = 250$. The lines are for negative vorticity with increment of 0.05 between contours (the first line represents -0.05). Each plot extends from $x = 25$ to 115 and $y = -7$ to 7. The time interval between frames corresponds to 400 time steps (9.8 time units).

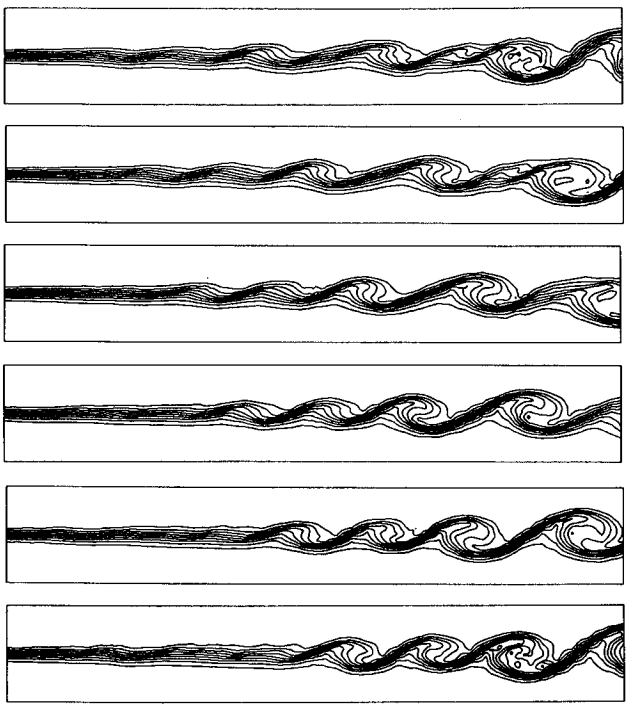

Fig. 4 Concentration contours for unforced case; $Re = 250$. Contour lines extend from 0.1 (bottom) to 0.9 (top) with increment of 0.1 between lines. Each plot extends from $x = 25$ to 115 and $y = -7$ to 7. The time interval between frames corresponds to 400 time steps (9.8 time units).

in character with occasional vortex pairing and formation of independent vortex lumps convected downstream. For this Reynolds number, the domain is too short for an effective transition to turbulence to take place.

Aligned with vortex formations in the shear layer is the formation of a mixing layer between the high-speed and low-speed fluids as shown in Fig. 4. As observed in experimental investigations, the fluid in the mixing layer prior to transition exists in three stages: tongues of unmixed freestream fluid, finite-thickness interfacial diffusion zones of mixed fluid, and cores of mixed fluid of nearly homogenous composition.[5] High gradient regions of concentration follow the outside perimeters of rolling vorticies and are convected downstream in concentrated lumps.

The time-averaged concentration contours (Fig. 5) indicate a uniformly growing average mixing region. A comparison between the temporal and averaged data emphasizes the limitations for practical applications of averaging, particularly in chemical processes or combustion where chemical rates have a nonlinear dependence on concentration.

Assuming the extent of the mixing layer as a region with concentration between 0.01 and 0.99, we extrapolate the boundaries of that region toward its origin, which in this case appears at $x_0 = -7$. We adopt this value as a reference in our attempts to seek similarities in mixing at all cross sections by substituting the y coordinate with $y/(x - x_0)$.

Plots of the average concentration profiles from four cross sections at $x = 15.2$, 45.2, 75.2, and 105.2 (Fig. 6) indicate that the concentration profiles are similar, with the exception of the first profile taken at a very close distance to the splitter plate edge, where the mixing as well as the velocity profiles are strongly affected by it.[22] The rms of concentration fluctuations (Fig. 6) shows steady asymmetric growth along the mixing layer with stronger effects on the low concentration side.

The average mixed-fluid concentration profiles (Fig. 6) are relatively steep compared with other studies.[6,7,25] This is primarily due to the influence of the splitter plate on the region of our interest[6] and to some extent the lower Schmidt number in our case. In the region next to the edge of the splitter plate,

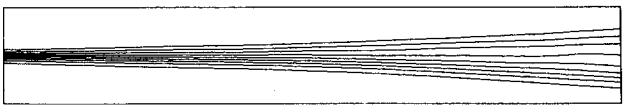

Fig. 5 Time-averaged concentration contours for unforced case; $Re = 250$. Contour lines extend from 0.1 (bottom) to 0.9 (top) with increment of 0.1 between lines. The plot is from $x = 25$ to 115 and $y = -7$ to 7.

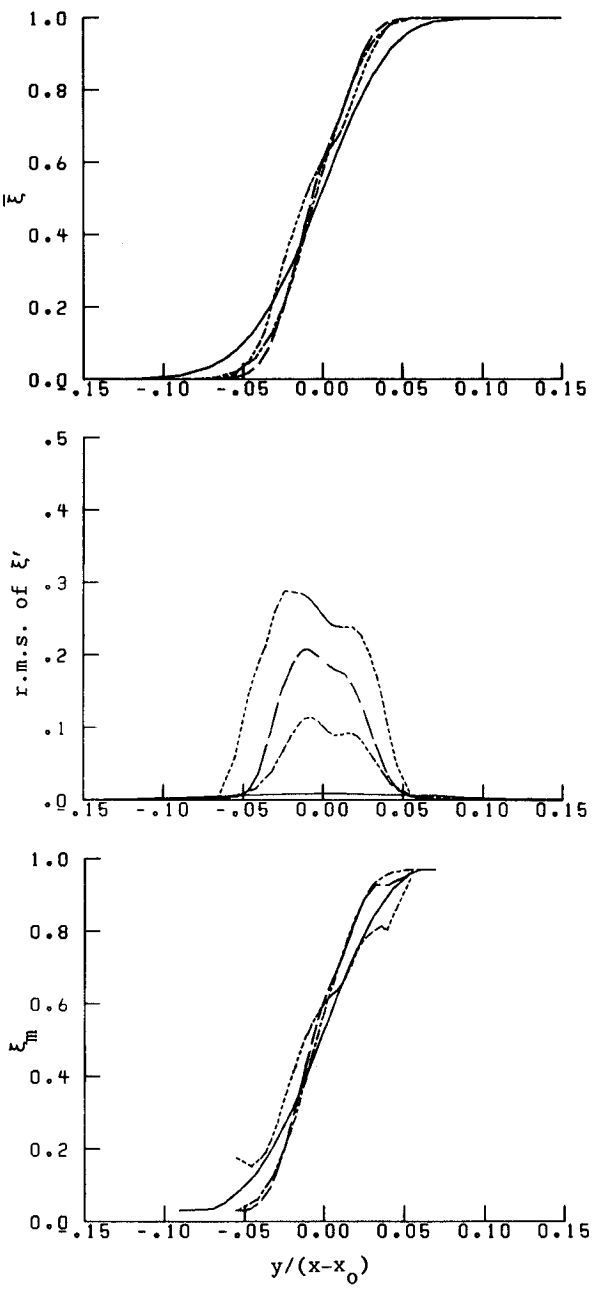

Fig. 6 Profiles of $\bar{\xi}$, rms of ξ', and ξ_m (average mixed-fluid concentration) for unforced case: $x = 15.2$, solid lines; 45.2, lines with dots; 75.2, dashed lines; 105.2, dots.

there is relatively little mixing, and that occurs at the thin interface separating the two fluids. The mixing, initially primarily by molecular diffusion, is increasingly augmented by convection due to growing vortex structures.

The increasing role of convective mixing in the downstream direction is apparent in the total mixed-fluid concentration shown in the Table 1. For the unforced case ($A_f = 0$), ξ_m is larger than 0.5 only at the very end of the domain. Similarly, the entrainment rate in our case (Table 2) is lower than unity,

Table 1 Total mixed-fluid concentration

		ξ_M			
A_f	f_f	$x = 15.2$	$x = 45.2$	$x = 75.2$	$x = 105.2$
0.005	0.058	0.470	0.478	0.511	0.534
0.0075	0.058	0.472	0.480	0.515	0.534
0.01	0.058	0.473	0.485	0.523	0.532
0.02	0.058	0.474	0.494	0.539	0.533
0.03	0.058	0.475	0.514	0.546	0.535
0.00	0.00	0.471	0.471	0.494	0.516
0.01	0.04	0.471	0.472	0.495	0.535
0.01	0.058	0.473	0.485	0.523	0.532
0.01	0.1	0.470	0.522	0.515	0.527
0.01	0.2	0.470	0.469	0.492	0.516

Table 2 Entrainment ratio

		E			
A_f	f_f	$x = 15.2$	$x = 45.2$	$x = 75.2$	$x = 105.2$
0.005	0.058	0.888	0.914	1.047	1.145
0.0075	0.058	0.893	0.923	1.062	1.144
0.01	0.058	0.898	0.944	1.094	1.137
0.02	0.058	0.899	0.977	1.170	1.143
0.03	0.058	0.905	1.058	1.202	1.148
0.00	0.00	0.891	0.890	0.975	1.064
0.01	0.04	0.890	0.892	0.979	1.153
0.01	0.058	0.899	0.944	1.094	1.137
0.01	0.1	0.888	1.094	1.060	1.115
0.01	0.2	0.887	0.884	0.968	1.067

with the exception of the region far downstream. These data indicate that the averaged mixing region in its initial formation and development is occupied equally by both fluids with increasing dominance of the high-velocity fluid toward downstream. The statistical data are based on the p.d.f. for the concentration of the high-velocity fluid. Figure 7 shows a representative sample of the p.d.f. at the last three cross sections of the mixing layer.

Mixing Enhancement by Forcing

At low Reynolds numbers, the mixing processes in shear layers require long distances to develop. Those processes can be intensified in many ways, for example, by introducing oscillatory forcing at inflow. It has been shown[22] the the character of the forcing component, that is, its amplitude and frequency, should be tuned with the unforced frequency response of the flowfield for maximum effects on the formation of vortex structures.

In our investigation the focus is placed on the influence of low-amplitude forcing, defined earlier by Eq. (3), added to the upper (high-speed) fluid velocity at inflow. With the unforced flow and concentration fields as initial conditions, two sets of simulations have been carried out: one for fixed frequency and varying amplitudes, the other for fixed amplitude and varying frequencies.

In the first set of simulations, the frequency has been chosen to be the most dominant frequency of the unforced flowfield (Fig. 2), $f_f = 0.058$, so that the forcing could create resonatory effects in the mixing layer. With the amplitudes of forcing chosen as $A_f = 0.005$, 0.0075, 0.01, 0.02, and 0.03, the overall effect of forcing amplitude variations is studied.

A closer look at one of the simulations for $A_f = 0.01$ demonstrates the typical behavior for all simulations in that group. Since the frequency has been chosen as the most dominant unforced response frequency, the excitation of the vortex structures in the layer is significant (Fig. 8) compared with the unforced case (Fig. 3). The vortex sheet becomes unsteady at a shorter distance[22] from the edge of the splitter plate, forming

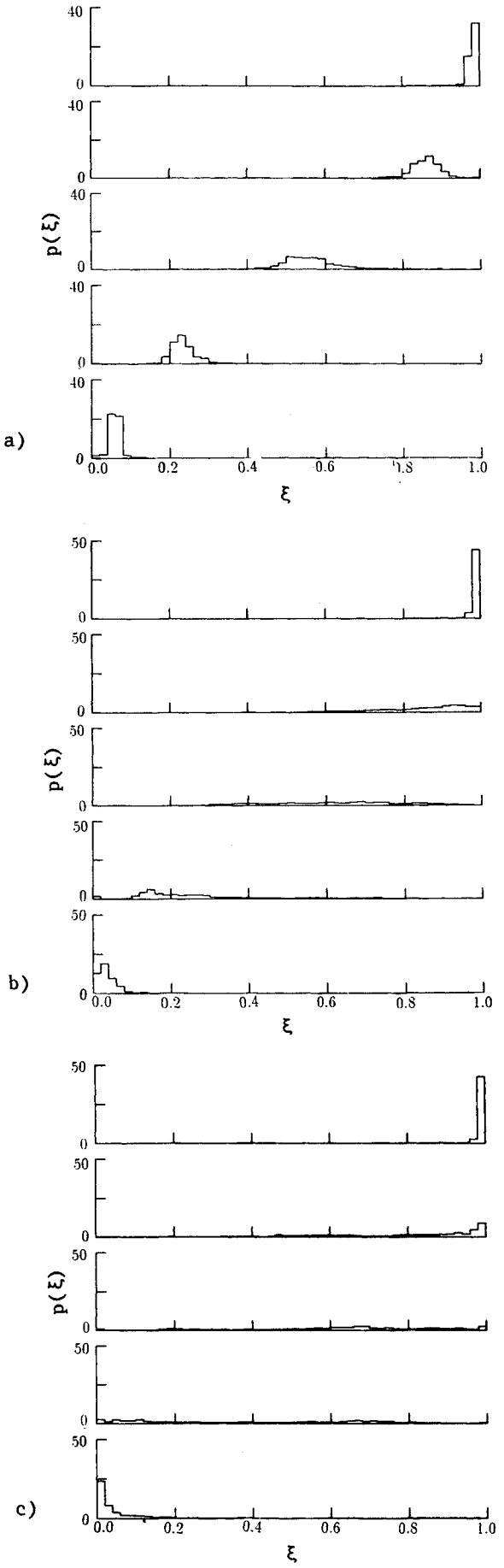

Fig. 7 Probability density function (unforced case) for ξ at $y/(x - x_0) = -0.04, -0.02, 0.0, 0.02$, and 0.04: cross section at a) $x = 45.2$; b) $x = 75.2$; c) $x = 105.2$.

vortex lumps that initially separate and then merge (pair) downstream into larger ones.

The effects of the above forcing are even more pronounced in the mixing of the upper and lower fluids as indicated in Fig. 9. After initial intensive roll ups of regions with high gradients of concentration on the outskirts of the vortical structures, the concentration contours show more structures (relatively low gradients) distribution far downstream. The averaged concentration contours (Fig. 10) indicate faster growth of the mixing layer at the initial length with rapidly growing vortex structures and slower growth of the mixing layer farther downstream. This behavior indicates that the flow is possibly approaching a transition stage from laminar to low-level turbulence.

The average concentration profiles (Fig. 11) indicate significant differences between mixing characteristics at different locations along the layer. The rms of concentration fluctuations (Fig. 11) shows a steady increase with downstream distance up to a point where the mixing layer becomes more uniform and the rms reaches its maximum. After that, the rms profile flattens out over the cross section. The average mixed-fluid concentration (Fig. 11), similar to the unforced case, is quite steep for reasons indicated for the unforced case given earlier. The typical form of the p.d.f. is shown on Fig. 12.

The influence of various amplitudes of forcing on the augmentation of mixing can be analyzed in terms of averaged quantities and by comparing temporal states of vortex and concentration structures in the domain. A comparison of the total mixed-fluid concentration ξ_M (Table 1, top) shows steady increase with growing amplitude. The slight decrease of ξ_M, followed by an increasing trend, for very low amplitudes at the far end of the domain is probably due to the diminishing role of the frequency matching far downstream. For very small amplitudes of oscillations, there might not be sufficient energy to sustain the enhanced (in the initial stage of the mixing layer) vortex structures.[22]

The entrainment ratio (Table 2, top) shows that the mixing layer becomes dominated by the high-speed fluid earlier than in the unforced case. The changes in the entrainment ratio as a function of amplitude follow those of the total mixed-fluid concentration discussed earlier.

A series of simulations with a constant amplitude of forcing, $A_f = 0.01$, and various frequencies demonstrate the dependence of the mixing enhancement on the frequency of outside forcing. Following the investigation in Ref. 22, the frequencies have been chosen based on the frequency spectrum of the unforced flow system (Fig. 2). The $f_f = 0.04$ Hz does not appear in the spectrum (Fig. 2) until far downstream, where it should give maximum enhancement due to resonance. Data in Tables 1 and 2 clearly show that this is indeed the case. The $f_f = 0.058$ Hz matches the dominant frequency in the unforced frequency spectrum and therefore should result in a maximum enhancement of mixing. Again, the data in both tables support that trend.

The two remaining simulations have been conducted with forcing frequencies that slightly match the unforced frequency spectrum only at the beginning of the mixing layer. It has been shown in Ref. 22 that forced excitation of shear layers with frequencies that do not match the unforced frequency spectra do not affect the developments of vortical structures unless the forcing amplitude is significant. As suspected, the enhancement of mixing follows the same trend. The data in Table 1 and 2 for the two cases given earlier show an increase in ξ_M and E in regions where matching of frequencies occur and no increase at all (with respect to the unforced case) for forcing with frequency totally outside of the unforced spectrum, as proven by the simulation with $f_f = 0.2$.

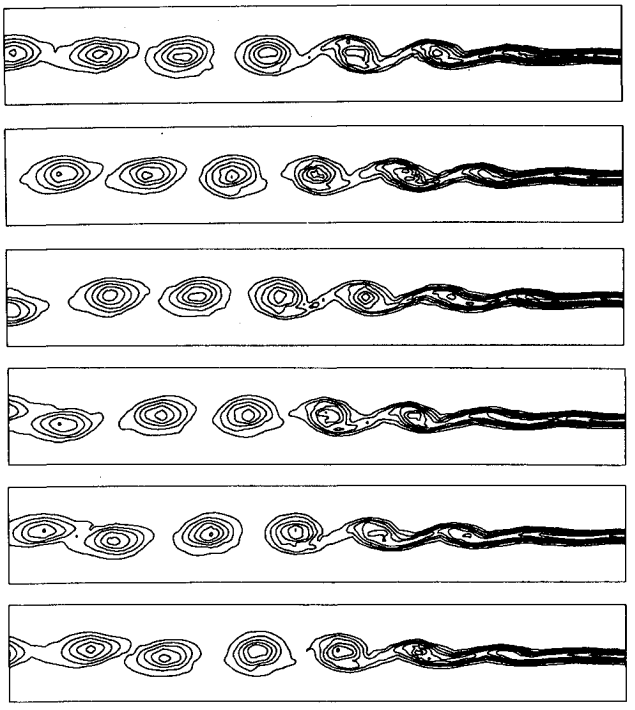

Fig. 8 Vorticity contours for forced case; $Re = 250$, $f_f = 0.057$, $A_f = 0.01$. The lines are for negative vorticity with increment of 0.05 between contours (the first line represents -0.05). Each plot extends from $x = 25$ to 115 and $y = -7$ to 7. The time interval between frames corresponds to 400 time steps (9.8 time units).

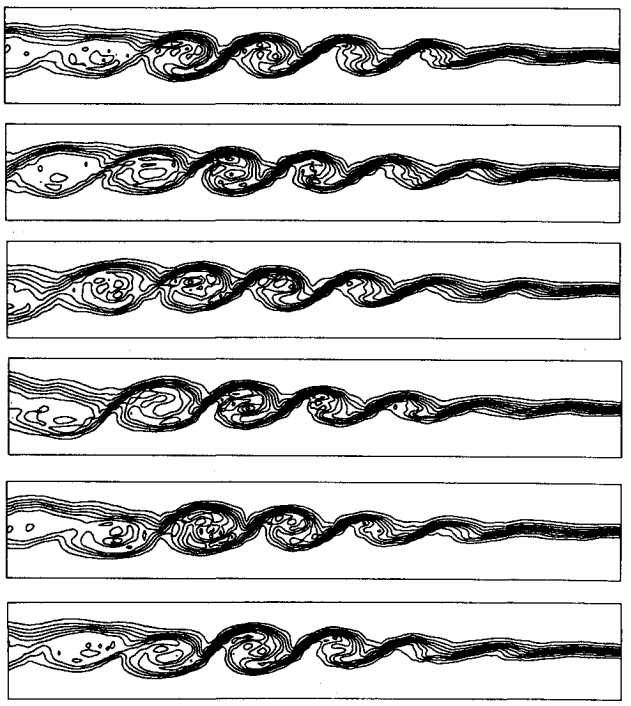

Fig. 9 Concentration contours for forced case; $Re = 250$, $f_f = 0.057$, $A_f = 0.01$. Contour lines extend from 0.1 (bottom) to 0.9 (top) with increment of 0.1 between lines. Each plot extends from $x = 25$ to 115 and $y = -7$ to 7. The time interval between frames corresponds to 400 time steps (9.8 time units).

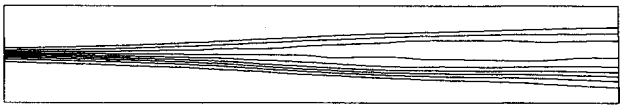

Fig. 10 Time-averaged concentration contours for forced case; $Re = 250$, $f_f = 0.057$, $A_f = 0.01$. Contour lines extend from 0.1 (bottom) to 0.9 (top) with increment of 0.1 between lines. The plot extends from $x = 25$ to 115 and $y = -7$ to 7.

For practical applications in chemical reactions, the averaged data might often be of limited use, whereas the temporal behavior of concentration variations could supply valuable insights. A brief comparison of concentration contours on Figs. 4, 9, and 13 reveals the dynamic structures of concentration changes. The forcing with frequencies that result in resonance significantly increases the dynamic mixing, as shown in Fig. 9 compared with Fig. 4. On the other hand, introduction of forcing with frequencies outside of the unforced frequency spectrum results in no noticeable effects on the averaged and dynamic changes in the mixing process, as seen by comparing Fig. 13 with Fig. 4.

Concluding Remarks

This investigation, by simulating the flow equations, represents a flow experiment carried out numerically. The flow, starting as laminar boundary layers over a splitter plate and undergoing transition in the mixing layer, is not restricted or

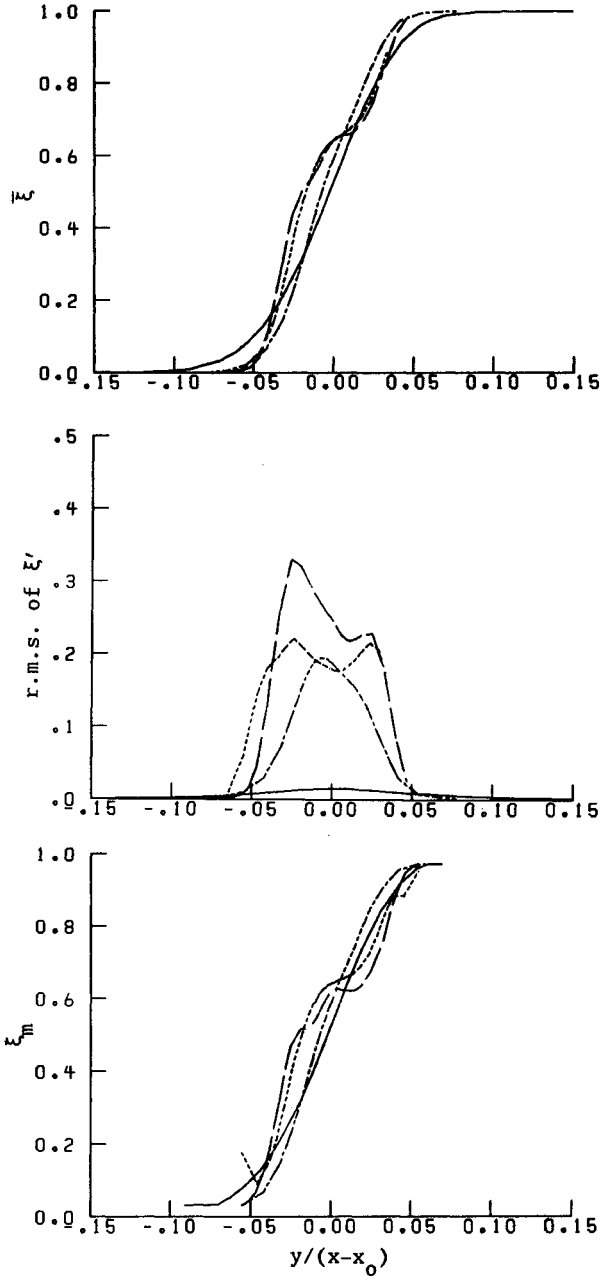

Fig. 11 Profiles of $\bar{\xi}$, rms of ξ', and ξ_m (average mixed-fluid concentration) for forced case: symbols as in Fig. 6.

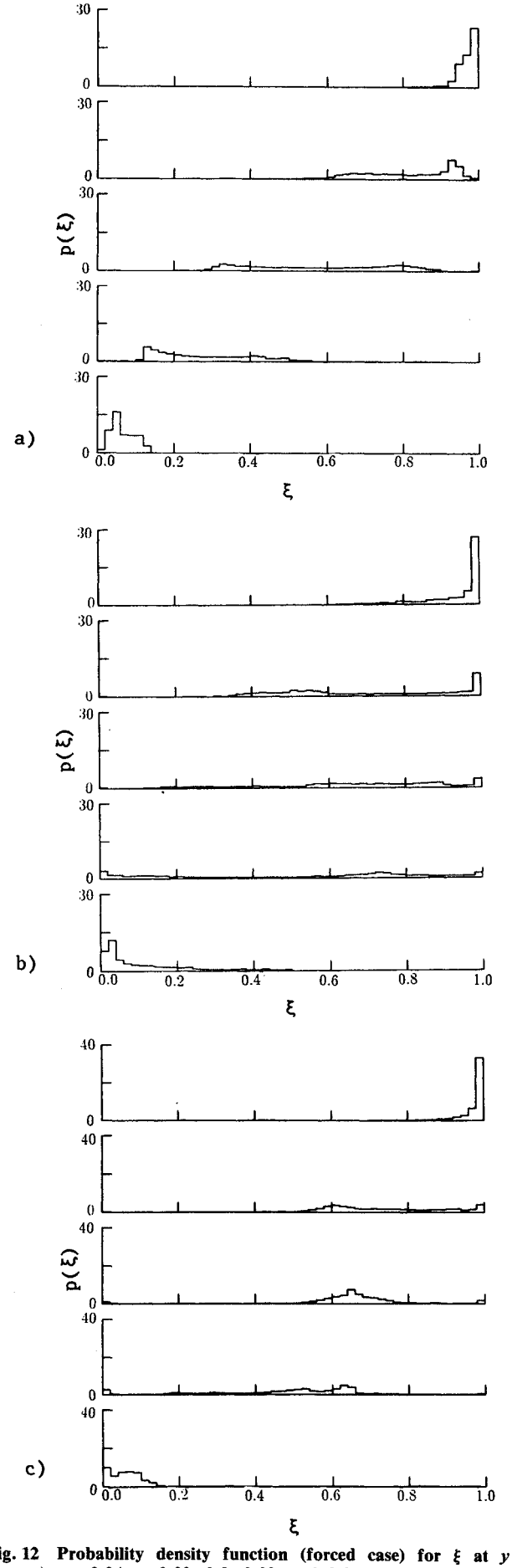

Fig. 12 Probability density function (forced case) for ξ at $y/(x - x_0) = -0.04, -0.02, 0.0, 0.02$, and 0.04: cross section at a) $x = 45.2$; b) $x = 75.2$; c) $x = 105.2$.

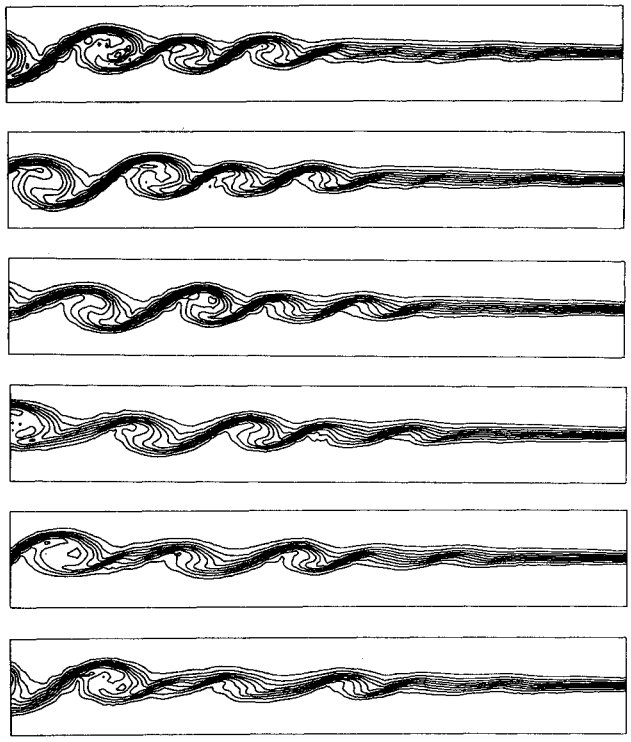

Fig. 13 Concentration contours for forced case; $Re = 250$, $f_f = 0.2$, $A_f = 0.01$. Contour lines extend from 0.1 (bottom) to 0.9 (top) with increment of 0.1 between lines. Each plot extends from $x = 25$ to 115 and $y = -7$ to 7. The time interval between frames corresponds to 400 time steps (9.8 time units).

predetermined by boundary or inflow conditions. In addition, a high-order (in all directions) solution algorithm ensures low numerical errors. These characteristics are essential for credible investigation of early developments in the layer.

The current study examines the influence of low-intensity outer oscillatory forcing on the enhancement of mixing. The simulations confirm the observed and intuitively expected result that increasing the amplitude of the forcing component results in mixing augmentation, both in terms of dynamic concentration changes and in terms of averaged quantities.

The simulations point out the importance of the forcing frequency selection for maximum mixing augmentation. The forcing frequency, adjusted in order to match an unforced dominant frequency in a specific region of a flow, results in significant local mixing enhancement. This could be used to control to some degree the mixing process. From a practical point of view, the important observation is that the addition of forced oscillations with incorrectly chosen frequencies has no noticeable effects on the development in the shear layer.

Thus far, all other numerical simulations dealing with mixing processes in plane shear layers were conducted without the splitter plate included in the computational domain and thus simplified the problem. In addition, experimental investigations rarely consider the formations in the vicinity of the splitter plate edge, instead concentrating on regions far downstream. As a result, we are able to make only fragmented and qualitative comparisons with the available data.

Acknowledgments

This investigation was supported by the Institute for Computational Mechanics in Propulsion, the NASA Graduate Student Researchers Program, and the Department of Mechanical and Aerospace Engineering at CWRU. Main computations were performed on the Cray XMP-28 at NASA Lewis Research Center.

References

[1]Miksad, R. W., "Experiments on the Nonlinear Stages of Free-Shear-Layer Transition," *Journal of Fluid Mechanics,* Vol. 56, Pt. 4, 1972, pp. 695-719.

[2]Winant, C. D. and Browand, F. K., "Vortex Pairing: The Mechanism of Turbulent Mixing-Layer Growth at Moderate Reynolds Number," *Journal of Fluid Mechanics,* Vol. 63, No. 2, 1974, pp. 237-255.

[3]Jimenez, J., "A Spanwise Structure in the Plane Shear Layer," *Journal of Fluid Mechanics,* Vol. 132, 1983, pp. 319-336.

[4]Oster, D. and Wygnanski, I., "The Forced Mixing Layer between Parallel Streams," *Journal of Fluid Mechanics,* Vol. 123, 1982, pp. 91-130.

[5]Masutani, S. M. and Bowman, C. T., "The Structure of a Chemically Reacting Plane Mixing Layer," *Journal of Fluid Mechanics,* Vol. 172, 1986, pp. 93-126.

[6]Koochesfahani, M. M. and Dimotakis, P. E., "Mixing and Chemical Reactions in a Turbulent Liquid Mixing Layer," *Journal of Fluid Mechanics,* Vol. 170, 1986, pp. 83-112.

[7]Konrad, J. H., "An Experimental Investigation of Mixing in Two-Dimensional Turbulent Shear Flows with Applications to Diffusion-Limited Chemical Reactions," Project SQUID TR-CIT-8-PU, 1976; also Ph.D. Thesis, California Institute of Technology, Pasadena, 1977.

[8]Bernal, L. P. and Roshko, A., "Streamwise Vortex Structure in Plane Mixing Layers," *Journal of Fluid Mechanics,* Vol. 170, 1986, pp. 499-525.

[9]Mungal, M. G. and Dimotakis, P. E., "Mixing and Combustion with Low Heat Release in a Turbulent Shear Layer," *Journal of Fluid Mechanics,* Vol. 148, 1984, pp. 349-382.

[10]Wygnanski, I. and Petersen, R. A., "Coherent Motion in Excited Free Shear Flows," AIAA Paper 85-0539, March 1985.

[11]Corcos, G. M. and Lin, S. J., "The Mixing Layer: Deterministic Models of a Turbulent Flow, Pt. 2: The Origin of the Three-Dimensional Motion," *Journal of Fluid Mechanics,* Vol. 139, 1984, pp. 67-95.

[12]Michalke, A., "On Spatially Growing Disturbance in an Inviscid Shear Layer," *Journal of Fluid Mechanics,* Vol. 23, 1965, pp. 521-544.

[13]Grinstein, F. F., Oran, E. S., and Boris, J. P., "Numerical Simulations of Asymmetic Mixing in Planar Shear Flows," *Journal of Fluid Mechanics,* Vol. 165, 1986, pp. 201-220.

[14]Gottlieb, D. O. and Orszag, S. A., "*Numerical Analysis of Spectral Methods: Theory and Application*, SIAM-CBMS, Philadelphia, 1977.

[15]Orszag, S. A. and Patterson, G. S., "Numerical Simulation of Turbulence," *Statistical Models and Turbulence,* Springer-Verlag, New York, 1972, pp. 127-147.

[16]Herring, J. R., Riley, J. J., Patterson, G. S., and Kraichnan, R. H., "Growth of Uncertainty in Decaying Isotropic Turbulence," *Journal of Atmospheric Science,* Vol. 30, No. 6, 1973, pp. 997-1006.

[17]Herring, J. R., "Approach of Axisymmetric Turbulence to Isotropy," *Physics of Fluids,* Vol. 17, No. 5, May 1974, pp. 859-872.

[18]Schumann, U. and Patterson, G. S., "Numerical Study of the Return of Axisymmetric Turbulence," *Journal of Fluid Mechanics,* Vol. 88, Pt. 4, 1978, pp. 711-735.

[19]Riley, J. J. and Metcalfe, R. W., "Direct Numerical Simulations of the Turbulent Wake of an Axisymmetric Body," *Turbulent Shear Flows,* Vol. 2, edited by L. J. S. Bradbury, et al., Springer-Verlag, Berlin, 1980, pp. 78-93.

[20]Riley, J. J. and Metcalfe, R. W., "Direct Numerical Simulation of a Perturbed, Turbulent Mixing Layer," AIAA Paper 80-0274, 1980.

[21]Metcalfe, R. W., Orszag, S. A., Brachet, M. E., Menon, S., and Riley, J. "Secondary Instability of a Temporally Growing Mixing Layer," *Journal of Fluid Mechanics,* Vol. 184, 1987, pp. 207-243.

[22]Korczak, K. Z. and Hu, D., "Turbulent Mixing Layers—Direct Spectral Element Simulation," AIAA Paper 87-0133, 1987.

[23]Riley, J. J. and Metcalfe, R. W., "Direct Simulations of Chemically Reacting Turbulent Mixing Layers," NASA CR-174640, March 1984.

[24]Lowery, P. S. and Reynolds, W. C., "Numerical Simulation of a Spatially-Developing, Forced, Plane Mixing Layer," NASA NCC-2-15, Rept. TF-26, Sept. 1986.

[25]Broadwell, J. W. and Breidenthal, R. E., "A Simple Model of Mixing and Chemical Reaction in a Turbulent Shear Layer," *Journal of Fluid Mechanics,* Vol. 125, 1982, pp. 397-410.

[26]Korczak, K. Z. and Patera, A. T., "An Isoparametric Spectral Element Method for Solution of the Navier-Stokes Equations in Complex Geometry," *Journal of Computational Physics,* Vol. 62, No. 2, Feb. 1986, pp. 361-382.